



# Paternal knockout of *Slc38a4*/SNAT4 causes placental hypoplasia associated with intrauterine growth restriction in mice

Shogo Matoba<sup>a,b,1</sup>, Shoko Nakamuta<sup>c</sup>, Kento Miura<sup>a</sup>, Michiko Hirose<sup>a</sup>, Hirosuke Shiura<sup>d</sup>, Takashi Kohda<sup>d</sup>, Nobuaki Nakamuta<sup>c</sup>, and Atsuo Ogura<sup>a,e,f,g,1</sup>

<sup>a</sup>Bioresource Engineering Division, Bioresource Research Center, RIKEN, 305-0074 Tsukuba, Ibaraki, Japan; <sup>b</sup>Cooperative Division of Veterinary Sciences, Tokyo University of Agriculture and Technology, 183-8509 Fuchu, Tokyo, Japan; <sup>c</sup>Faculty of Agriculture, Iwate University, 020-8550 Morioka, Iwate, Japan; <sup>d</sup>Faculty of Life and Environmental Sciences, University of Yamanashi, 400-8510 Kofu, Yamanashi, Japan; <sup>e</sup>Graduate School of Life and Environmental Sciences, University of Tsukuba, 305-8572 Tsukuba, Ibaraki, Japan; <sup>f</sup>The Center for Disease Biology and Integrative Medicine, Faculty of Medicine, University of Tokyo, 113-0033 Tokyo, Japan; and <sup>g</sup>Bioresource Engineering Laboratory, RIKEN Cluster for Pioneering Research, 351-0198 Wako, Saitama, Japan

Edited by Janet Rossant, Hospital for Sick Children, University of Toronto, Toronto, ON, Canada, and approved September 6, 2019 (received for review May 8, 2019)

The placenta is critical in mammalian embryonic development because the embryo's supply of nutrients, including amino acids, depends solely on mother-to-embryo transport through it. However, the molecular mechanisms underlying this amino acid supply are poorly understood. In this study, we focused on system A amino acid transporters *Slc38a1*/SNAT1, *Slc38a2*/SNAT2, and *Slc38a4*/SNAT4, which carry neutral, short-side-chain amino acids, to determine their involvement in placental or embryonic development. A triple-target CRISPR screen identified *Slc38a4*/SNAT4 as the critical amino acid transporter for placental development in mice. We established mouse lines from the CRISPR founders with large deletions in *Slc38a4* and found that, consistent with the imprinted paternal expression of *Slc38a4*/SNAT4 in the placenta, paternal knockout (KO) but not maternal KO of *Slc38a4*/SNAT4 caused placental hypoplasia associated with reduced fetal weight. Immunostaining revealed that SNAT4 was widely expressed in differentiating cytotrophoblasts and maturing trophoblasts at the maternal-fetal interface. A blood metabolome analysis revealed that amino acid concentrations were globally reduced in *Slc38a4*/SNAT4 mutant embryos. These results indicated that SNAT4-mediated amino acid transport in mice plays a major role in placental and embryonic development. Given that expression of *Slc38a4* in the placenta is conserved in other species, our *Slc38a4*/SNAT4 mutant mice could be a promising model for the analysis of placental defects leading to intrauterine growth restriction in mammals.

amino acid transporter | SNAT | placental development | IUGR | metabolome

The placenta supports normal embryonic development and growth during pregnancy in mammals. The most critical function of the placenta is to transport nutrients, gases, and waste materials between the maternal and fetal circulations to ensure the appropriate environment required for embryonic development in the uterus (1). The maternal and fetal circulations are physically separated by several layers of cells/membranes; thus, transfer of molecules across these layers is precisely controlled by factors that are present at the maternal-fetal interface (2). Defects in placental function can cause various abnormalities of embryogenesis, including intrauterine growth restriction (IUGR) and miscarriage (1, 3). Moreover, a poor nutritional environment during the embryonic period has been suggested to have long-term effects on the metabolic programs of offspring, even in postnatal life (4). Therefore, poor functioning of the placenta is believed to be problematic not only for embryogenesis but also for adult life. Despite their tremendous importance, the molecular mechanisms underlying placental functions, including efficient nutritional transport, are poorly understood.

The nutrients that are transferred from mother to fetus across the placenta include glucose, fatty acids, and amino acids. Of these, amino acids are key molecules that support embryonic development

(5). Because the plasma concentration of each amino acid is generally higher in the fetal circulation than in the maternal circulation, amino acids are thought to be actively transported across the maternal-fetal barrier (6). In fact, the human placenta expresses over 20 amino acid transporters (7).

System A amino acid transporters make up one of the best studied systems in the placenta. System A amino acid transporters comprise 3 small neutral amino acid transporters (SNATs), *Slc38a1*/SNAT1, *Slc38a2*/SNAT2, and *Slc38a4*/SNAT4, which are characterized by their Na<sup>+</sup>-dependent transfer activity, with a preference for small neutral amino acids such as alanine, serine, and glutamine (8). SNAT4 exhibits properties that are different from those of the other members of this family, including lower activity for neutral amino acids and acceptance of cationic amino acids such as histidine (9, 10). The placenta in both humans and rodents expresses all 3 SNAT genes (11–13). Because system A amino acid transporters can transport the nonmetabolizable amino acid analog MeAIB, its incorporation in human placenta-derived syncytiotrophoblasts or their cytoplasm (microvillus membrane [MVM] vesicles) has been extensively used to study system A activities in the placenta (9, 13–16). Importantly, many studies

## Significance

Although it has been suggested that system A amino acid transporters are involved in mammalian placental or embryonic development, most studies in this field have relied on in vitro experiments using primary cells/cytoplasts from human placentas. The present study provides genetic evidence of the developmental roles of system A amino acid transporters and identifies *Slc38a4*/SNAT4 as being critical to embryonic and placental development in mice. In addition, a blood metabolome analysis provides unequivocal evidence that *Slc38a4*/SNAT4 plays a key role in the supply of amino acids to the fetus. These results provide insights into the link between genetic alterations and the nutritional environment of the fetus, which may affect its development to term.

Author contributions: S.M. and A.O. designed research; S.M., S.N., K.M., M.H., H.S., T.K., and N.N. performed research; S.M., S.N., K.M., N.N., and A.O. analyzed data; and S.M. and A.O. wrote the paper.

The authors declare no competing interest.

This article is a PNAS Direct Submission.

Published under the PNAS license.

Data deposition: The microarray data have been deposited in the NCBI Gene Expression Omnibus (GEO; <https://www.ncbi.nlm.nih.gov/geo/>), under accession no. GSE136212.

<sup>1</sup>To whom correspondence may be addressed. Email: shogo.matoba@riken.jp or atsuo.ogura@riken.jp.

This article contains supporting information online at [www.pnas.org/lookup/suppl/doi:10.1073/pnas.1907884116/-DCSupplemental](http://www.pnas.org/lookup/suppl/doi:10.1073/pnas.1907884116/-DCSupplemental).

First published September 30, 2019.

using the MeAIB incorporation assay have described a correlation between reduced system A activity and IUGR in humans (14–16). An association between *Slc38a4* overexpression in the placenta and human fetal macrosomia has also been reported (17). However, there is no definitive in vivo genetic evidence of SNAT gene involvement in placental amino acid transfer.

In this study, we examined the developmental functions of SNAT genes via CRISPR-based genetic screening in a mouse model. We also examined the detailed developmental phenotypes and the metabolic consequences of SNAT gene knockout (KO) using established deletion lines derived from the CRISPR founders. Our study provides genetic evidence of the critical role of *Slc38a4*/SNAT4 in placental and embryonic development.

## Results

**System A Amino Acid Transporters Are Highly Expressed in the Developing Placenta.** To understand the dynamic expression patterns of SNAT genes in different tissues in mice, we performed reverse transcription quantitative PCR (RT-qPCR) using tissues of adult mice and term fetal (E19.5) mice (*SI Appendix, Fig. S1 A–C*). Although in adults *Slc38a1* and *Slc38a2* were broadly expressed in a wide range of tissues, *Slc38a4* was almost exclusively expressed in the liver, which is consistent with the results of previous reports (18, 19). A comparison of the expression levels of SNAT genes in tissues of term fetuses and placentas revealed that all 3 SNAT genes were expressed at high levels in the placenta (*SI Appendix, Fig. S1 A–C*). We then examined their dynamic expression patterns in the developing placenta and embryos, and found that the expression levels of these genes were higher in extraembryonic tissues than they were in embryonic tissues, at least from E7.5 to term (*SI Appendix, Fig. S1 D–F*). Specifically, at E11.5 or earlier, *Slc38a1* and *Slc38a2* but not *Slc38a4* were highly expressed in Reichert's membrane (i.e., the parietal wall of the mouse yolk sac). Importantly, expression levels of the SNAT genes in the placenta increased as development proceeded. These results indicate that all SNAT genes are highly expressed in the extraembryonic tissues or placenta, suggesting that they play critical roles in mouse placental development.

**Triple-Target CRISPR Screen Identifies *Slc38a4*/SNAT4 as a Critical Transporter in Placental Development.** To determine whether any of the SNAT genes play a critical role in placental development in mice, we performed a triple-target CRISPR screen, a technique that allows the production of whole-body homozygous KO founder mice directly from zygotes at a very high efficiency (20, 21). We designed 3 single-guide RNAs (sgRNAs) targeting distinct protein-coding exons for each gene. The 3 sgRNAs, each targeting a SNAT genes, were injected together with the *Cas9* mRNA into in vitro fertilized (IVF) zygotes with a C57BL/6N (B6N) inbred background to produce biallelic KO mice of each gene separately (*SI Appendix, Fig. S2A*). After transfer of these embryos into the oviduct of pseudopregnant females, we examined their phenotypes at term after cesarean section (*SI Appendix, Fig. S2B*). The implantation rates did not differ between the control and experimental groups (*SI Appendix, Fig. S2C*). Founder pups were delivered at similar rates in the 3 triple-target CRISPR-injected groups (*SI Appendix, Fig. S2D*). Interestingly, we found that placental weight was significantly reduced only in the group of embryos injected with sgRNAs targeting *Slc38a4* (sgSlc38a4; 69% of the control group) (Fig. 1A). The body weight of the sgSlc38a4 embryos was also significantly reduced, to 75% of the control value (Fig. 1B). sgSlc38a4 pups frequently died shortly after birth, and only 5 of 18 delivered pups survived to 2 wk (28% survival). Despite the normal size of their placentas (Fig. 1A), sgSlc38a1 and sgSlc38a2 embryos were slightly but significantly smaller than control embryos (Fig. 1B). Next, we examined the histology of sgSlc38a4 placentas by hematoxylin and eosin (HE) staining and found that both the spongiotrophoblast (ST)

and labyrinth (LB) layers were significantly smaller in sgSlc38a4 placentas compared with controls (Fig. 1C and *SI Appendix, Fig. S2E*). Analysis of the expression of SNAT genes by RT-qPCR confirmed that the target genes were specifically reduced in each triple-target CRISPR founder placenta (*SI Appendix, Fig. S2F*). These results suggest that, among the SNAT-family genes, *Slc38a4*/SNAT4 plays the most critical role in mouse placental development.

**Paternal Deletion of *Slc38a4*/SNAT4 Causes Placental Hypoplasia and Reduced Fetal Weight.** Next, we investigated the detailed developmental phenotypes of *Slc38a4* mutants. Although the triple-target CRISPR approach is a powerful method of in vivo screening, it has several limitations, especially for dissecting precise mechanisms and detailed phenotypes during development, because of the variable patterns of mutation in different founders. To overcome these limitations, we established KO lines from the triple-target CRISPR founder mice that contained a total deletion of the coding regions of the *Slc38a4* gene. We found that 2 out of 5 surviving founder mice (#9 and #12) possessed the required large-deletion alleles (*SI Appendix, Fig. S3A*) and had deletions of ~23 kb (*SI Appendix, Fig. S3B*). Importantly, each allele had a deletion of a different length, which enabled us to distinguish the parental origin of the mutant alleles by PCR after mating. We mated the founders that harbored deletion alleles with wild-type (WT) B6N mice and established 3 lines of *Slc38a4* deletion mutants (#9-A, #12-B, and #12-C) (*SI Appendix, Fig. S3C*).

*Slc38a4* exhibits imprinted paternal expression in various embryonic tissues and in the placenta in mice (18, 19). In fact, sequencing of transcripts in a B6N × JF1 hybrid placenta at term revealed that *Slc38a4* was dominantly expressed from the paternal allele in mouse placenta (paternal 68% vs. maternal 32%). While mating the founders to establish the deletion lines, we noticed that, consistent with this imprinting pattern, the inheritance of the deletion alleles from the father but not from the mother caused severe placental hypoplasia and low birth weight. Importantly, similar phenotypes were consistently observed in all 3 deletion lines (*SI Appendix, Fig. S3 D and E*). The natural mating of heterozygous maternal knockout (MKO) males and MKO females produced pups with a normal litter size and a ratio of each genotype (WT, MKO, paternal KO [PKO], null) that followed the Mendelian ratio, at least until term (*SI Appendix, Table S1*). PKO and Null pups showed a similar placental hypoplasia and reduced birth weight (*SI Appendix, Fig. S3 F and G*). Because IVF using MKO males and MKO females followed by embryo transfer also generated mutant embryos in a similar ratio (*SI Appendix, Table S1*), we used IVF-generated embryos for the latter analysis.

At term, the placenta in PKO mice was significantly smaller than that in WT mice (Fig. 2A and *SI Appendix, Fig. S3 H–J*), with a placental weight that was 41% lower than that of WT mice, while MKO placentas were of normal weight. Body weight was also 33% lower in PKO compared with WT mice (Fig. 2B and *SI Appendix, Fig. S3H*). Importantly, these phenotypes were observed at similar levels in the homozygous mutants (Null) (45% decrease in placental weight; 25% decrease in body weight) (Fig. 2A and B). Consistent with the imprinting pattern of *Slc38a4*, a gene expression analysis performed at E13.5 and E19.5 using RT-qPCR revealed that the expression of *Slc38a4* was greatly reduced (>80%) in PKO placentas and slightly reduced (20–32%) in MKO placentas compared with WT placentas (*SI Appendix, Fig. S3 K and L*). In the fetal liver, the reduction in *Slc38a4* expression levels in PKO samples was less obvious (58%) at term, while it was clearer at E13.5 (69%) (*SI Appendix, Fig. S3 M and N*). Of note, the *Slc38a4* PKO/Null pups frequently died during the postnatal growth period, typically within 1–2 d after birth (*SI Appendix, Fig. S3O*); consequently, at 3 wk the population ratio was strongly biased toward the WT and MKO genotypes (*SI Appendix, Fig. S3P*). Moreover, the body size of the surviving PKO or Null mice

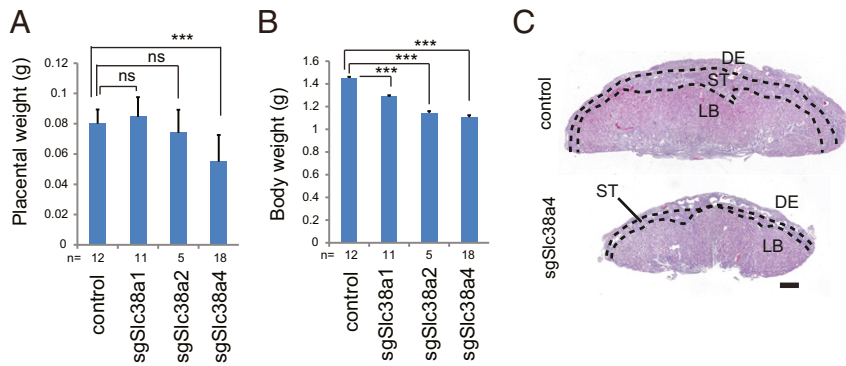


**Fig. 1.** Triple-target CRISPR screen identifies *Slc38a4* as an amino acid transporter that is critical in placental development. (A) Placental weight of founder mice at E19.5. ns, not significant.  $***P < 0.001$ . (B) Body weight of founder mice at E19.5.  $***P < 0.001$ . (C) Representative images of placental sections stained by HE. DE, decidua; ST, spongiotrophoblast layer; LB, labyrinthine layer. (Scale bar, 500  $\mu\text{m}$ .)

remained consistently smaller than that of the WT or MKO mice until adulthood (*SI Appendix, Fig. S3Q*). These results suggest that paternal inheritance of the *Slc38a4* KO allele causes severe placental hypoplasia associated with reduced fetal weight in mice, which is a phenotype similar to that of the triple-target CRISPR founders.

**Reduction in the LB and ST Layers in *Slc38a4* PKO/Null Placentas.** To determine the time at which the placental phenotype of *Slc38a4* mutants began to appear, we analyzed the *Slc38a4* mutant embryos at E11.5, E13.5, and E16.5. We found that the reduction in placental weight in PKO and Null embryos became obvious at E13.5 (35% and 37%, respectively) (Fig. 2A). This phenotype appeared to initiate as early as E11.5, although the reduction in placental weight was not significant at that stage (Fig. 2A). In contrast, body

weight reduction in PKO and Null embryos did not become apparent until E16.5 (Fig. 2B), suggesting that placental defects precede the small-body phenotype.

To determine which layer of the placenta was responsible for the placental size reduction in *Slc38a4* mutants, we analyzed the histology of *Slc38a4* mutant placentas via periodic acid Schiff (PAS) staining, which turns the glycogen-positive ST layer purple. PKO and Null placentas showed reduced total areas at E13.5 (Fig. 2C and *SI Appendix, Fig. S4A*). While the area of the ST layer appeared normal in PKO/Null placentas at E13.5, the LB layer was already significantly smaller in PKO/Null placentas vs. WT placentas at E11.5 (Fig. 2C and *SI Appendix, Fig. S4 B and C*). The ST layer was reduced in PKO/Null placentas after E16.5. These results suggest that paternal inheritance of the *Slc38a4* KO allele causes poor development of the LB layer as early as E11.5 and

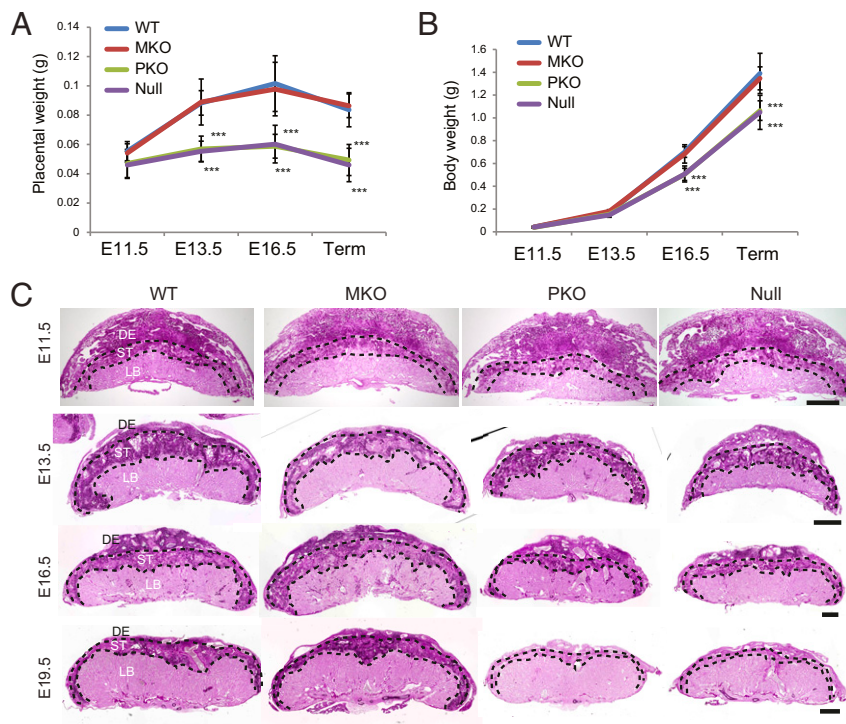


**Fig. 2.** Paternal deletion of *Slc38a4/SNAT4* causes placental hypoplasia and intrauterine growth restriction. (A) Placental weight during embryonic development. Note that the placental weight is significantly lower in PKO and Null embryos starting at E13.5.  $***P < 0.001$ . (B) Body weight during embryonic development. Note that body weight reduction in PKO or Null embryos appears after E13.5.  $***P < 0.001$ . (C) Histological images of PAS-stained placentas at E11.5, E13.5, E16.5, and E19.5. DE, decidua; ST, spongiotrophoblast layer; LB, labyrinth layer. (Scale bar, 500  $\mu\text{m}$ .)



that this small LB layer is maintained throughout the subsequent stages of development. Reduction in the ST layer is likely secondary to the deficiency in the LB layer.

To understand the effect of *Slc38a4* depletion on gene expression patterns in the placenta, we performed a microarray analysis using E13.5 placentas with biological duplicates. Among the 30,391 probes that were detected consistently in all samples, 280 and 651 probes were commonly up-regulated or down-regulated (fold change >2), respectively, in PKO/Null mice; moreover, they were unchanged in MKO animals (Datasets S1 and S2). Importantly, *Slc38a4* was the top down-regulated gene in Null samples (Dataset S2 and *SI Appendix, Fig. S5A*). The expression levels of placental lineage markers, such as *Cdx2*, *Tpbpa*, *Gcm1*, and *Cd34*, were not significantly changed in the mutant placenta (fold change <2) (*SI Appendix, Fig. S5A*), suggesting that *Slc38a4* KO did not significantly affect lineage differentiation in the placenta, at least at this stage. A gene ontology analysis revealed that, while no category was enriched in the up-regulated genes, the down-regulated genes were significantly enriched for cell cycle-related terms (*SI Appendix, Fig. S5B*). These results suggest that PKO/Null placentas may have proliferation defects.

**Dynamic Expression Patterns of SNAT4 Proteins in the Developing Placenta.** To understand precisely the function of SNAT4 in the developing placenta, we performed immunohistochemical staining for SNAT4 in the placenta at different stages from E10.5 to term. At E10.5, SNAT4 was expressed in both the ST and LB layers, with expression being highest in chorionic basal trophoblast populations (arrows in Fig. 3A). Concomitantly, SNAT4 was expressed at the maternal–fetal interface (arrowhead in Fig. 3A). This broad distribution pattern was observed until E13.5, although SNAT4 expression in ST cells increased gradually. Interestingly, from E13.5 onward, SNAT4 expression diminished in chorionic basal trophoblast populations and in the ST layer but was maintained at the maternal–fetal interface (Fig. 3A). These results suggest that SNAT4 plays diverse roles during placental development.

**SNAT4 Is Expressed in Trophoblasts in the Chorionic Plate to Support Their Proliferation.** Based on the observation that SNAT4 was highly expressed in the basal chorionic plate (CP) in E10.5 placentas and that the reduction in LB layer size in PKO/Null placentas appeared as early as E11.5, we investigated whether the paternal KO of *Slc38a4* caused cell proliferation defects in chorionic trophoblast cells. Because the CP is formed at around E8.5, we first analyzed SNAT4 protein localization at E8.5, at which stage SNAT4 was broadly expressed in the extraembryonic regions, including the ectoplacental cone (EPC) and the CP (Fig. 3B). We confirmed that SNAT4 was depleted in PKO and Null placentas. It is noteworthy that a small population of cells in PKO placentas expressed SNAT4, suggesting a leaky expression of *Slc38a4* from the maternal allele (*SI Appendix, Fig. S4D*). Such leaky expression of *Slc38a4*/SNAT4 was similarly observed in natural mating–derived PKO embryos (*SI Appendix, Fig. S4E*). We then analyzed cell proliferation via phosphohistone H3 (pHH3) staining, which labels dividing cells at the M phase. At E8.5, the number of pHH3-positive cells was significantly reduced in the CP of PKO placentas while that in the EPC, which forms the ST layer at later stages, was similar to that observed in WT placentas (Fig. 3B–D). This reduced proliferation of chorionic trophoblasts and their derivative labyrinthine trophoblast cells was observed throughout development until E13.5 (Fig. 3C and *SI Appendix, Fig. S6A*). Consistent with such delayed proliferation, CP attachment to the EPC appeared to be delayed in PKO and Null embryos (Fig. 3B). In contrast, cleaved caspase 3, which is a marker of apoptosis, was rarely observed in any genotype at these stages (*SI Appendix, Fig. S6B*). Thus, the small placental LB layer observed in *Slc38a4* PKO/Null placentas was likely caused by the poor proliferation of chorion-derived trophoblast cells rather than EPC-derived trophoblast cells.

The ST area was significantly reduced in PKO or Null placentas starting at E16.5 (Fig. 2C and *SI Appendix, Fig. S4C*). The ST layer consists of spongiotrophoblasts and glycogen cells. We found that the intensity of PAS staining, an indicator of glycogen, was diminished in the PKO/Null ST layer (Fig. 2C). A transmission electron microscopy (TEM) analysis confirmed that glycogen particles were rarely found in presumptive glycogen cells of PKO and Null placentas (*SI Appendix, Fig. S7A*). Moreover, immunostaining for Cdx2, which showed glycogen cell–specific staining in the ST layer, indicated that the number of glycogen cells was greatly reduced at E19.5 (*SI Appendix, Fig. S7B and C*). Interestingly, at E16.5 many glycogen cells were positive for pHH3 in WT/MKO placentas, whereas such signals were greatly reduced in PKO and Null placentas (Fig. 3D and *SI Appendix, Fig. S6C*). These results suggest that the reduction in the ST layer detected in *Slc38a4* PKO animals was caused by a combination of reduced proliferation and exhaustion of stored glycogen in the ST glycogen cells likely because of a poor nutritional environment.

**SNAT4 Is Expressed in SynT-II to Support the Efficient Transfer of Amino Acids to the Fetal Circulation.** In addition to the chorionic trophoblasts, SNAT4 was expressed in the LB layer of the maternal–fetal interface (Fig. 3A). The maternal–fetal interface in mice is a hemochorial barrier that comprises layers of different cell types as follows (from the fetal to the maternal side): fetal endothelial cells that surround fetal blood vessels, basement membrane, 2 syncytiotrophoblast layers (SynT-I and SynT-II), and sinusoidal trophoblast giant cells (sTGCs), which face the maternal blood circulation directly (2). Costaining with markers for SynT-I (Mct1) and SynT-II (Mct4) revealed that SNAT4 was colocalized with Mct4 but not with Mct1 (Fig. 4A). SNAT4 signals were closely associated with expression of the basement membrane marker laminin, which is located between SynT-II and fetal endothelial cells (Fig. 4A). Thus, SNAT4 was expressed in the SynT-II cells adjacent to the basement membrane.

We examined structural changes in the maternal–fetal interface in *Slc38a4* mutant placentas by staining for CD34, which is a marker of endothelial cells; however, we did not observe any significant changes in the morphology of the interface (*SI Appendix, Fig. S8A*). A TEM analysis revealed that the normal layers of the maternal–fetal interface appeared to be maintained in PKO or Null placentas (*SI Appendix, Fig. S8B*). These results suggest that the structure of the maternal–fetal interface is normal in *Slc38a4* mutants.

Considering its function as an amino acid transporter, SNAT4 likely contributes to the transfer of amino acids to the fetal circulation at the maternal–fetal interface. Thus, we examined the nutritional consequences for fetal blood circulation of the absence of SNAT4. We collected blood plasma samples from *Slc38a4* mutants at term (WT,  $n = 4$ ; PKO,  $n = 3$ ; Null,  $n = 3$ ) and performed a capillary electrophoresis time-of-flight mass spectrometry (CE-TOFMS) metabolome analysis to capture the nutritional status of the embryos. By comparing the relative concentrations of the 253 molecules detected in this analysis between WT and PKO or Null mice (Dataset S3), we identified 3 molecules that were significantly up-regulated and 11 molecules that were significantly down-regulated in the plasma of PKO and Null mice (Fig. 4B). Among them, hypotaurine was the most significantly and consistently down-regulated in PKO (34% of WT) and Null (22% of WT) plasma (Fig. 4B). Interestingly, the 11 down-regulated molecules included 3 amino acids: isoleucine, glutamine, and histidine. Thus, we focused our analysis on all 20 amino acids and found that, in PKO or Null plasma, the majority of amino acids were significantly down-regulated and that none were up-regulated (Fig. 4C). Consistent with such reduction in amino acid concentrations, a pathway enrichment analysis of our metabolome datasets indicated that amino acid transport–related categories were highly enriched in the changed molecules (*SI Appendix, Fig. S9A*). We also performed the metabolome analysis using blood plasma of sgSlc38a1, sgSlc38a2, and sgSlc38a4 founder pups and found that concentration







